A Robust Observer-Based Method for IGBTs and Current Sensors Fault Diagnosis in Voltage-Source Inverters of PMSM Drives

Imed Jlassi, Jorge O. Estima, *Member, IEEE*, Sejir Khojet El Khil, Najiba Mrabet Bellaaj, and Antonio J. Marques Cardoso, *Senior Member, IEEE*

***Abstract*—Permanent magnet synchronous motors (PMSMs) drives using three-phase voltage-source inverters (VSIs) are currently used in many industrial applications. The reliability of VSIs is one of the most important factors to improve the reliability and availability levels of the drive. Accordingly, this paper presents a robust fault diagnostic method for multiple insulated gate bipolar transistors (IGBTs) open-circuit faults and current sensor faults in three-phase PMSM drives. The proposed observer-based algorithm relies on an adaptive threshold for fault diagnosis. Current sensor and open-circuit faults can be distinguished and the faulty sensors and/or power semiconductors are effectively isolated. The proposed technique is robust to machine parameters and load variations. Several simulation and experimental results using a vector-controlled PMSM drive are presented, showing the diagnostic algorithm robustness against false alarms and its effectiveness in both IGBTs and current sensors fault diagnosis.**

***Index Terms*—Condition monitoring, fault diagnosis, IGBTs and current sensors faults, permanent magnet machines, voltage-source inverter (VSI).**

NOMENCLATURE

$i_{\rm sk}$	Measured three-phase PMSM currents.
$\hat{i}_{\rm sk}$	Observed three-phase PMSM currents.
$\varepsilon_{\rm sk}$	Observed error.
F_k	Measured currents form factor of phase *k*.
$\hat{F}_k$	Observed currents form factor of phase *k*.
r_k	PMSM residual values of phase *k*.
T_k	PMSM adaptive thresholds of phase *k*.
T_o	PMSM fixed threshold.
I_s	PMSM currents sum.
ω_r	PMSM rotor speed.
$x_{skAv}, x_{sk\rm RMS}$	Average, RMS values of variable *x*.

Manuscript received June 6, 2016; revised August 15, 2016; accepted September 18, 2016. Date of publication October 11, 2016; date of current version May 18, 2017. Paper 2016-IDC-0380.R1, approved for publication in the IEEE TRANSACTIONS ON INDUSTRY APPLICATIONS by the Industrial Drives Committee of the IEEE Industry Applications Society. This work was supported by the Portuguese Foundation for Science and Technology under Project SFRH/BPD/87135/2012 and Project SFRH/BSAB/118741/2016.

I. Jlassi and S. K. El Khil are with the Université de Tunis El Manar, Ecole Nationale d'Ingénieurs de Tunis, Laboratoire des Systèmes Electriques, LR11ES15, 1002, Tunis, Tunisia, and also with CISE—Electromechatronic Systems Research Centre, 6201-001, Covilhã, Portugal (e-mail: jlassi-imed@hotmail.fr; sejirkek@gmail.com).

J. O. Estima and A. J. M. Cardoso are with CISE—Electromechatronic Systems Research Centre, Universidade da Beira Interior 6201-001, Covilhã, Portugal (e-mail: jestima@ieee.org; ajmcardoso@ieee.org).

N. M. Bellaaj is with the Université de Tunis El Manar, Ecole Nationale d'Ingénieurs de Tunis, Laboratoire des Systèmes Electriques, LR11ES15, 1002, Tunis, Tunisia (e-mail: najiba_bm@yahoo.fr).

Color versions of one or more of the figures in this paper are available online at http://ieeexplore.ieee.org.

Digital Object Identifier 10.1109/TIA.2016.2616398

I. INTRODUCTION

CURRENTLY, permanent magnet synchronous motor (PMSM) drives using three-phase voltage-source inverters (VSIs) are used in a variety of industrial applications and processes. Power converters present complex conversion systems that are often exposed to high stresses, which make them susceptible to several failures [1]. Industry statistical results presented in [2] and [3] show that power converter faults are the most common in variable speed drives. Other statistical results addressed in [4], [5], and [8] show that a very high percentage (≈53%) of failures in power converters are attributed to control circuits.

Power semiconductor faults are broadly classified as short-circuit faults and open-circuit faults [5], [8]. They are caused by high electrical or thermal stresses, gate driver failure, or wire disconnection. Short-circuit faults are the most dangerous and may damage the inverter. This type of fault can lead to an abnormal overcurrent that can cause damage to other components. Consequently, in order to achieve fast fault detection, converters are equipped with specific hardware protection circuits. Another way to deal with short-circuit faults is the use of fast fuses. In this case, short-circuit faults become open-circuit faults. Open-switch faults are characterized by a current imbalance in both faulty and healthy phases which causes a pulsating torque. Such a fault may cause secondary damage to other components and may even cause the shutdown of the drive. Therefore, condition monitoring and fault diagnosis are considered effective tools in order to increase the reliability and availability levels of variable speed drive systems. Apart from failures occurring in the power semiconductors, the drive is also sensitive to failures in the sensors that provide information used by the main control system. Since closed loop controls are mandatory in order to achieve high performances, an erroneous feedback given by these sensors may put in risk the control system operation, which may lead to secondary faults in other components and dangerous scenarios. Typically, in PMSM drives, the sensors

measure three-phase currents, dc-link voltage, and rotor position. Sensor failures are broadly classified as sensor gain drop, sensor measurement with offset, intermittent sensor connection, or complete sensor outage. The latter two are the most severe faults, since they imply a momentary or complete lack of information which is used by the main control system [6]. Therefore, real-time sensors fault detection is strongly recommended [7].

For this reason, fault diagnostic methods have been developed during the last years in order to overcome this problem. Several insulated gate bipolar transistors (IGBTs) fault diagnostic methods can be found in the literature [8]–[11].

There are different ways to classify open-circuit fault detection and isolation (FDI) approaches. The literature review shows that they may be classified as current signatures [12]–[20], [22]–[25], [30], [33]–[36] and voltage signatures based methods [26]–[29], [31], [32]. Also for such faults, methodologies can be classified into model-based [21]–[25], [29]–[36] and model-free methods [12]–[20], [26]–[28]. A more detailed classification following the methodologies applied can also be considered.

Signal processing methods using motor currents like average current method [10]–[12] and current slope analysis [13], [14] have the advantage that they are free of machine or inverter models and load transients. However, they still require relatively long time to achieve fault detection and identification (almost 1.5–2 current fundamental periods) and have serious problems under low-current values. Current similarity analysis for open-circuit fault diagnosis in the three-phase PWM rectifier is presented in [15]. Authors propose to detect 21 types of faults. However, this method is still complex to implement with high tuning effort.

Artificial-intelligence-based approaches like neural network [16], fuzzy network [17], [12], and wavelet based methods [18]–[20] allow smart diagnosis with no need of a system model. Nevertheless, their drawbacks are that their high computational requirements considerably increase the detection time and make them complex for real-time implementation.

Park's vector approach was proposed in [14] and [21]–[23], allowing for the open-circuit fault diagnostic in the power converters. A novel approach for single open-circuit fault diagnostic in VSIs for PMSM drives was proposed for multiple faults diagnosis in [22]. In [21], a comparison of different Park's approaches is presented. The literature [23] uses the error between motor currents and their references to achieve real-time multiple open fault diagnosis in voltage-fed PWM motor drives. However, this algorithm cannot be applied to open loop control strategies. In [24] and [25], Park's vector approach is associated with a pattern recognition approach for multiple open-circuit fault detection in ac drives.

Voltage-based techniques developed and proposed in [26]–[29] allow fast detection time and good performance. But they require using additional sensors, which increase the system complexity and cost.

More recently, the observer-based method has been proposed for FDI purposes [30]–[36]. Voltage estimators are applied in [31] and [32]. Different types of current observers such as Luenberger state observer, nonlinear observers, or proportional integral observers are employed [30], [33]–[36]. These methods perform good diagnosis with relatively short detection time. As they are based on residual generation, they are sensitive to motor parameters variations. For these methods, the threshold selector is still the key issue to insure effective and robust diagnosis.

Regarding the occurrence of sensors faults in the drive, some research works have also been conducted. In [37] and [38], offset and scaling errors of the current measurement in a machine drive were analyzed and compensated, allowing for the machine operation with minimal torque ripple. In [39]–[42], some diagnostic techniques, as well as system reconfigurations, were proposed for sensors faults in doubly fed induction generator drives. Luenberger observers are used in [39] and [40] to provide residuals for fault diagnosis. In [41], the current sensor fault detection is obtained by comparing the absolute value of the sum of the three currents with normalized thresholds. The analysis of the current error vector in a field programmable gate array implementation of hysteresis current control was addressed in [42] to diagnose current sensor failures. In [43], the fault detection is achieved by using a parity space approach. Some techniques are proposed in [44]–[47] for detection and isolation of several sensor types, namely current, voltage, and speed sensors. In [44], current and voltage sensors fault diagnosis algorithm as well as system reconfigurations are proposed using Luenberger observer and residual generation. The literature [45] provides offline current fault diagnosis using a state observer. An adaptive observer is proposed to estimate the motor phase currents in [46], and the faulty sensor localization uses a deterministic rule, which takes some electrical cycles, in practice. The extended Kalman filter is proposed in [47] for sensor diagnostic purposes, as well as to achieve fault tolerance with respect to speed sensor faults [48], [49]. Estimator approaches were presented in [50] for speed and current sensor fault diagnosis and fault tolerance, allowing for the drive continuous operation. Average normalized currents methods are applied to detect sensor fault detection in [51] and [52].

The literature review shows that fault diagnostic techniques developed and proposed for power electronics and motor drives faults are based on detection thresholds, which have an impact on the robustness of these techniques. Indeed, fixed thresholds need adjustments according to the operating point modification and parameters model uncertainty. Due to the use of constant thresholds, the robustness of these algorithms can be reduced. On the other side, the state of the art review also shows that power semiconductors and current sensor fault diagnosis in power electronics and variable speed drives are two issues that were classically treated separately. Typically two algorithms are developed for diagnostic purposes: one for power switch faults and the second for current sensor failures.

So, best known to the authors, no work has been reported toward a unique FDI structure for multiple IGBTs open-circuit and a current sensors fault in ac drives. In case of the use of a unique structure for different types of faults, the use of fixed threshold will increase the tuning effort and the proposed approach will be much more complex to implement. As a result, adaptive thresholds become very interesting [53]. Moreover, such a generalized FDI approach would be beneficial in more complex systems including three-phase two-level converters.

Accordingly, this paper presents a single diagnostic method based on adaptive thresholds, for multiple IGBTs open-circuit

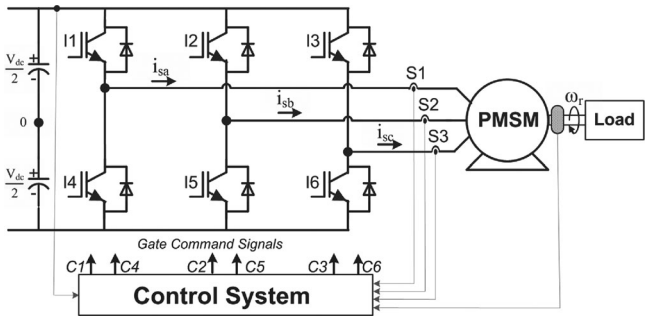

Fig. 1. Block diagram of the PMSM drives system.

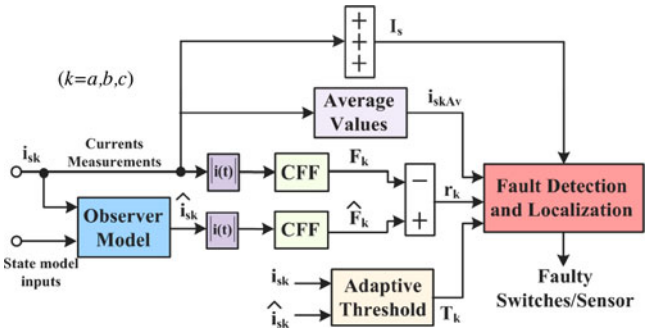

Fig. 2. Block diagram of the fault diagnostic technique.

faults and current sensors faults in VSIs of PMSM drives. The considered current sensors failures are those that lead to a complete sensor outage, due to the supply failure or the sensor disconnection. The proposed method is a state observer-based one with an adaptive threshold approach, which can guarantee a reliable diagnosis under distinct system operating points and different faulty operating modes. The proposed algorithm only requires the information given by current sensors and the quantities already available from the main control, avoiding the use of any additional sensors which results in further costs and complexity on the system. Simulation and experimental results are presented, showing the algorithm performance regarding the diagnostic of power semiconductor faults and current sensor faults under distinct operating conditions such as different load levels and speed values.

II. Proposed Fault Diagnosis Algorithm

Fig. 1 shows a three-phase VSI with six IGBTs and their respective antiparallel diodes, feeding a PMSM. A closed-loop vector control system is considered, in order to achieve high PMSM drive performances.

The schematic block diagram of the proposed fault diagnostic method is depicted in Fig. 2. The proposed FDI algorithm is based on the current form factor (CFF) and adaptive thresholds, calculated from the measured motor phase currents and the estimated currents. The Luenberger state observer is used in order to estimate the motor currents. First, two CFFs are calculated for each motor phase: F_k from the measured current and $\hat{F}_k$ through the estimated current $(k = a, b, c)$. Second, three residues r_k are generated, based on the difference between F_k and $\hat{F}_k$. Then, adaptive thresholds T_k are established based on residues r_k. Next, the comparison between each residual and their corresponding adaptive threshold allows for the fault detection. Current sensor faults and IGBTs open-circuit faults can be distinguished by using the currents sum I_s. Finally, in case of IGBT faults, the current average values i_{skAv} associated with the faulty leg help to identify the faulty switches.

A. Luenberger Observer for the Motor Currents

The current Luenberger observer was proposed in [36], for multiple IGBTs open-circuit faults diagnosis in back-to-back converters of PMSG drives for wind turbine systems. In this paper, the main objective of the Luenberger observer is to estimate the three-phase motor currents. Therefore, the derived state space model is the basis for the observer to estimate the inverter's output currents.

The PMSM current dynamic model can be represented as follows:

$$\underbrace{\begin{pmatrix} \frac{di_{\mathrm{sd}}}{dt} \\ \frac{di_{\mathrm{sq}}}{dt} \end{pmatrix}}_{\dot{x}} = \underbrace{\begin{pmatrix} -\frac{R_s}{L_s} & -w_r \\ w_r & -\frac{R_s}{L_s} \end{pmatrix}}_{A} \underbrace{\begin{pmatrix} i_{\mathrm{sd}} \\ i_{\mathrm{sq}} \end{pmatrix}}_{x} + \underbrace{\begin{pmatrix} \frac{1}{L_s} & 0 \\ 0 & \frac{1}{L_s} \end{pmatrix}}_{B} \underbrace{\begin{pmatrix} V_{\mathrm{sd}} \\ V_{\mathrm{sq}} \end{pmatrix}}_{u} + \underbrace{\begin{pmatrix} 0 \\ -\frac{\psi_{\mathrm{PM}} w_r}{L_s} \end{pmatrix}}_{De}. \quad (1)$$

The general state space model is given by

$$\begin{cases} \dot{x}(t) = Ax(t) + Bu(t) + De(t) \\ y(t) = Cx(t) \end{cases} \quad \text{where } C = (1\ 1). \quad (2)$$

The Luenberger state-observer equations are given by

$$\begin{cases} \dot{\hat{x}}(t) = A\hat{x}(t) + Bu(t) + De(t) + L(y(t) - \hat{y}(t)) \\ \hat{y}(t) = C\hat{x}(t) \end{cases}. \quad (3)$$

The state correction vector $L(y(t) - \hat{y}(t))$ presents the difference between the measured and the observed quantities, where L is 2×2 matrix given by

$$L = \begin{pmatrix} L_1 & L_3 \\ L_4 & L_2 \end{pmatrix}. \quad (4)$$

The matrix gains are chosen in order to define the observer dynamics. Accordingly, the observer dynamic error is defined by the eigenvalues of the matrix $(A - LC)$. These eigenvalues should be selected according to the system requirements, which are, typically, rapid response and stable and accurate current estimation as follows:

$$\det(sI - (A - LC)) = (s - \lambda_1)(s - \lambda_2) = 0. \quad (5)$$

By solving (5), it can be obtained:

$$s^2 + f_c(L_1, L_2)s + g_c(L_1, L_2, L_3, L_4) = 0 \quad (6)$$

where

$$\begin{cases} f_c(L_1, L_2) = 2\frac{R_s}{L_s} + L_1 + L_2 \\ g_c(L_1, L_2, L_3, L_4) = \left(\frac{R_s}{L_s} + L_1\right)\left(\frac{R_s}{L_s} + L_2\right) \\ \qquad\qquad + (w_r + L_3)(w_r - L_4) \end{cases}. \quad (7)$$

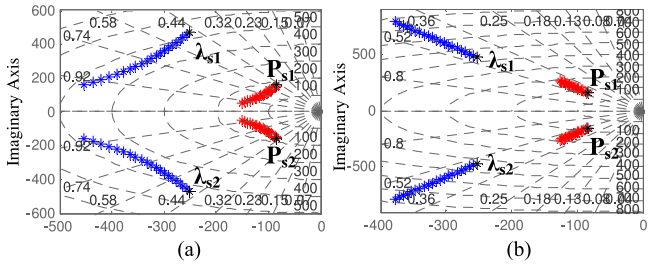

Fig. 3. System and observer eigenvalues (a) in case of stator inductance and speed variations and (b) in case of stator resistance and speed variations.

The observer eigenvalues are given by

$$\lambda_{s1,s2} = \frac{-f_c(L_1, L_2)}{2} \pm j\frac{1}{2}\sqrt{f_c(L_1, L_2)^2 - 4g_c(L_1, L_2, L_3, L_4)}. \quad (8)$$

The observer dynamics are fixed by the real parts of the eigenvalues $\lambda_{s1,s2}$. Thus, L_3 and L_4 values are supposed to be null. When the real part of the eigenvalues assumes large negative values, the observer error converges rapidly. Choosing the eigenvalues too aggressively, however, results in amplification of the system noise and degraded or even unstable performance. The desired $\lambda_{s1,s2}$ locations are enforced through the selection of the gains L_1 and L_2.

Another factor that impacts the eigenvalues selection strategy is the evolution of the observed error. This error can be reduced by choosing observer eigenvalues $\lambda_{s1,s2}$ to impose faster observer dynamics compared to the system poles $P_{s1,s2}$ as follows:

$$\begin{cases} \mathrm{Re}(\lambda_{s1,s2}) = n.\mathrm{Re}(P_{s1,s2}) \\ \mathrm{Im}(\lambda_{s1,s2}) = m.\mathrm{Im}(P_{s1,s2}) \end{cases} \quad (9)$$

where n and m are chosen according to the desired observer dynamics. Therefore, L_1 and L_2 values are selected by choosing the values of n and m.

In Fig. 3, the dynamics of the observer is imposed in order to evaluate the evolution of eigenvalues and the robustness of the state observer, under the PMSM stator parameters and the rotor speed variations. Fig. 3(a) shows that all observer eigenvalues have a negative real part for stator inductance L_s variation from 70% to 100% of its rated value and rotor speed ω_r variation from 35% to 100% of its rated value, meaning that the observer remains stable for all the considered variations. Fig. 3(b) shows that the observer stays stable for a variation of stator resistance R_s from 100% to 150% of its rated value simultaneously with rotor speed ω_r variation from 35% to 100% of its rated value.

B. Residual Generation and Adaptive Threshold Definition

Two CFFs are calculated for each phase: one from the measured current and the other through the estimated current:

$$F_k = \frac{|i_{\mathrm{sk}}|_{\mathrm{RMS}}}{|i_{\mathrm{sk}}|_{\mathrm{Av}}}, \quad \hat{F}_k = \frac{\left|\hat{i}_{\mathrm{sk}}\right|_{\mathrm{RMS}}}{\left|\hat{i}_{\mathrm{sk}}\right|_{\mathrm{Av}}} \quad \text{where } k = a, b, c. \quad (10)$$

For each phase, a residual is generated and can be expressed as follows:

$$r_k = \hat{F}_k - F_k. \quad (11)$$

For the healthy case and in steady-state operating mode, the three values of CFFs, corresponding to each phase current, are approximately equal to 1.111. Thus, each residual r_k should be equal to zero. However, due to operating point variations, PMSM parameters model variation, or measurement noises, the residual will be around zero. Therefore, a comparison of each residual to a threshold is necessary.

An adaptive threshold is established through the expression of residuals. According to (11), residuals r_k can be expressed as follows:

$$r_k = \frac{|i_{\mathrm{sk}} + \varepsilon_{\mathrm{sk}}|_{\mathrm{RMS}}}{|i_{\mathrm{sk}} + \varepsilon_{\mathrm{sk}}|_{\mathrm{Av}}} - \frac{|i_{\mathrm{sk}}|_{\mathrm{RMS}}}{|i_{\mathrm{sk}}|_{\mathrm{Av}}} \quad (12)$$

where $\varepsilon_{\mathrm{sk}}$ is the observed error given by

$$\varepsilon_{\mathrm{sk}} = \hat{i}_{\mathrm{sk}} - i_{\mathrm{sk}}. \quad (13)$$

These residuals can be majored as follows:

$$r_k \leq \frac{|i_{\mathrm{sk}}|_{\mathrm{RMS}}}{|i_{\mathrm{sk}} + \varepsilon_{\mathrm{sk}}|_{\mathrm{Av}}} + \frac{|\varepsilon_{\mathrm{sk}}|_{\mathrm{RMS}}}{|i_{\mathrm{sk}} + \varepsilon_{\mathrm{sk}}|_{\mathrm{Av}}} - \frac{|i_{\mathrm{sk}}|_{\mathrm{RMS}}}{|i_{\mathrm{sk}}|_{\mathrm{Av}}}. \quad (14)$$

According to the previous equation, the observer error $\varepsilon_{\mathrm{sk}}$ is neglected when compared to the value of i_{sk}. Thus, the adaptive threshold can be expressed by

$$T_k = \frac{|\varepsilon_{\mathrm{sk}}|_{\mathrm{RMS}}}{|i_{\mathrm{sk}}|_{\mathrm{Av}}}. \quad (15)$$

The evolution of the threshold T_k depends on the dynamics of the estimation error and the motor operating point variation. The estimation error $\varepsilon_{\mathrm{sk}}$ depends on the dynamics of the estimated currents. Gains L_1 and L_2 are selected in order to define the current observer dynamics, and therefore, the correct threshold is obtained by the good choice of L_1 and L_2 values. It is clear that the residual value of each phase always stays below its corresponding adaptive threshold T_k under normal operating conditions, independent of current transients or speed variations.

C. Fault Detection and Localization

Fault detection and localization can be accomplished using Table I. Current sensor faults and IGBTs open-circuit faults detection is performed by analyzing the evolution of each residual against their corresponding adaptive thresholds. Under the healthy mode, residuals r_k are lower than their corresponding thresholds T_k, independent of the operating conditions. However, when a fault occurs in the current sensor or in an inverter power switch, the residual associated with the faulty device will exceed its corresponding threshold, indicating therefore the existence of a fault in that phase.

After the fault detection, the IGBT open-circuit fault is distinguished from the current sensor fault by using the sum of the three-phase motor currents, given by

$$I_s = i_{\mathrm{sa}} + i_{\mathrm{sb}} + i_{\mathrm{sc}}. \quad (16)$$

TABLE I
IGBT OPEN-CIRCUIT FAULTS AND CURRENT SENSOR FAULTS DIAGNOSIS ON THREE-PHASE VOLTAGE-SOURCE INVERTERS

Faulty Device		Detection variables			Currents Sum	Localization variables		
		r_a	r_b	r_c		i_{saAv}	i_{sbAv}	i_{scAv}
IGBT	I1	$>T_a$			$I_s = 0$	$<-T_o$	X	X
	I4	$>T_a$				$>T_o$	X	X
	I2		$>T_b$			X	$<-T_o$	X
	I5		$>T_b$			X	$>T_o$	X
	I3			$>T_c$		X	X	$<-T_o$
	I6			$>T_c$		X	X	$>T_o$
	I1,I4	$>T_a$				$\in[-T_o,T_o]$	X	X
	I2,I5		$>T_b$			X	$\in[-T_o,T_o]$	X
	I3,I6			$>T_c$		X	X	$\in[-T_o,T_o]$
	I1,I5	$>T_a$	$>T_b$			$<-T_o$	$>T_o$	X
	I2,I4	$>T_a$	$>T_b$			$>T_o$	$<-T_o$	X
	I1,I6	$>T_a$		$>T_c$		$<-T_o$	X	$>T_o$
	I3,I4	$>T_a$		$>T_c$		$>T_o$	X	$<-T_o$
	I2,I6		$>T_b$	$>T_c$		X	$<-T_o$	$>T_o$
	I3,I5		$>T_b$	$>T_c$		X	$>T_o$	$<-T_o$
Sensor	S1	$>T_a$			$I_s \neq 0$	X	X	X
	S2		$>T_b$			X	X	X
	S3			$>T_c$		X	X	X

Note: X means that the current average values are not used.

Under an IGBT open-circuit fault, the currents sum I_s is always equal to zero, whereas the current sensor fault in the motor phases causes a nonbalanced three-phase current system, resulting in oscillating currents sum.

Regarding the IGBT open-circuit fault, the residuals signatures present the same result in the case of a single or double IGBT open-circuit fault in the same leg. Thus, the residuals allow only the detection and the isolation of the faulty leg, but cannot identify the damaged IGBT. In this case, the diagnostic algorithm uses the current average values i_{skAv} associated with the faulty legs, in order to identify the damaged power switches. In addition, a fixed threshold value T_o can be used to confirm the localization of the faulty semiconductor. It should be mentioned that a single power switch open-circuit fault in the upper or bottom IGBT in the same leg causes the exceeding of values $-T_o$ or $+T_o$, respectively; whereas, when a double IGBT open-circuit fault occurs in the same leg, the current average value associated with the faulty leg takes values within the range $\pm T_o$. The value of T_o is fixed by analyzing the current average values under the healthy case and different faulty operating modes.

III. SIMULATION RESULTS

The PMSM drive model comprises basically a three-phase VSI connected to a 2.2 kW PMSM, with the parameters shown in Table II. A rotor-field-oriented control (RFOC) is combined with a space vector modulation (SVM) technique, and applied to the inverter. The modeling and simulation of the PMSM drive system as well as of the proposed fault diagnostic algorithm were carried out using the MATLAB Simulink environment. IGBT open-circuit faults are applied by removing their corresponding gate command signals and current sensor faults are introduced by forcing their output signals to zero.

TABLE II
PARAMETERS OF THE USED PMSM

Power	P	2.2 kW
Speed	N	1750 r/min
Voltage	V	316 V
Current	I	5.3 A
Torque	T_L	12 N·m
Frequency	f	145.8 Hz
Armature resistance	R_s	1.72 Ω
Magnet flux linkage	Ψ_{PM}	0.244 Wb
d/*q*-axis inductance	$L_{\mathrm{sd/q}}$	20.5 mH

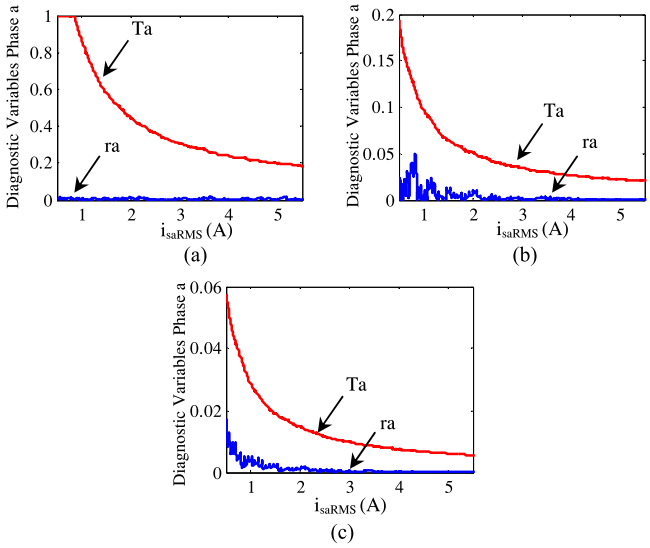

Fig. 4. Diagnostic variables according to the observer dynamic variations. (a) $L_1 = L_2 = 1000$, (b) $L_1 = L_2 = 8000$, and (c) $L_1 = L_2 = 40\,000$.

A. Thresholds Selection

The thresholds selection is empirically established in order to accommodate high transients and to perform the fault detection in a wide range of operating conditions. Thus, a large threshold increases the diagnostic method robustness but also increases the detection time. For a very large threshold, the method will not be able to detect the fault. On the contrary, a small threshold not only decreases the detection time but also decreases the algorithm robustness, especially for a very small threshold, since false alarms can be generated.

Taking into account that the motor is fed by a healthy inverter generating a perfectly balanced three-phase sinusoidal current system, different matrix gains L_1 and L_2 were tested in order to select the correct adaptive threshold. Fig. 4 presents the diagnostic variables of phase "a" versus observer gains (L_1 and L_2) variations, under a time-varying load and considering a reference speed of 600 r/min. Under low-load operating conditions, the current is small and presents a significant harmonic distortion, resulting in more oscillating diagnostics variables. The increasing of load torque causes the increasing of the current amplitude and the decreasing of the harmonic distortion, resulting in more stable diagnostic variables.

Fig. 4(a) shows that small L_1 and L_2 values cause low observer dynamics, resulting in a very large threshold, especially

at low-current values. Therefore, the proposed algorithm is not capable of performing the fault detection under these operating conditions. In Fig. 4(b), a good separation is obtained between the residual r_a and its corresponding adaptive threshold T_a, in a wide range of operating conditions, meaning that the matrix gains $L_1 = L_2 = 8000$ can be used for diagnostic purposes, independent of the system operating points, which can guarantee a fast observer dynamics, assuring effective diagnostics and avoiding false alarms.

Fig. 4(c) shows that very large L_1 and L_2 values cause very fast observer dynamics, resulting in a very small threshold, and thus, false alarms may occur, especially at larger current values. It should be noticed that the obtained results for the diagnostic variables dedicated to the phases "b" and "c" are very similar to the previous ones shown in Fig. 4, since the conditions are the same. Therefore, the previous analysis is also valid in this case.

Regarding the IGBT fault localization, the value of threshold T_o is chosen by analyzing the current average values under healthy and faulty operating conditions. Therefore, under normal operation and under a double IGBT open-circuit fault in the same phase, the current average values are between +0.2 and –0.2 A; whereas, a single open-circuit fault in the upper or bottom IGBT causes the exceeding of the value –0.2 or +0.2 A, respectively. This means that the value 0.2 A can be used for T_o, assuring a good localization performance.

B. Multiple IGBTs and Current Sensors Faults Diagnosis

Fig. 5 presents the simulation results regarding the motor currents together with the variables used to perform fault diagnostic, during load transients and a fault occurrence in the inverter leg, with an imposed reference speed of 600 r/min.

Three load steps are introduced. At $t = 1.3$ s, the load torque decreases from 67% of the rated load torque to 34%. After that, at $t = 1.4$ s, the load torque reduces again to 16% of the rated value. Under healthy operating conditions and during the load transients, it can be seen that all residuals r_k stay always below their corresponding adaptive thresholds T_k and no false alarms are generated. Therefore, the immunity to false alarms resulting from load variations is verified.

With the aim to evaluate the diagnostic performance under faulty operating conditions, a power switch open-circuit fault is applied in IGBT *I*1 at the instant $t = 1.508$ s. As the opened power switch *I*1 corresponds to the upper IGBT in the inverter phase "a," the current in this phase will only take negative values. This fault also has a negative impact on the currents of the healthy phases, leading to the increase in currents and higher harmonic distortion, imposing greater Joule losses and thermal stresses in the motor windings, together with large shaft mechanical stresses. Regarding the fault diagnostic, the *I*1 fault is localized at the instant $t = 1.513$ s, corresponding to 25% of the motor currents period, when the residue r_a crosses their threshold T_a, the currents sum I_s remains zero and the value of i_{saAv} becomes less than –*T*. It is visible that all the other residues corresponding to the healthy phases remain far away from their thresholds for these operating conditions. The simulation results presented in Fig. 6 address the diagnostic algorithm capability

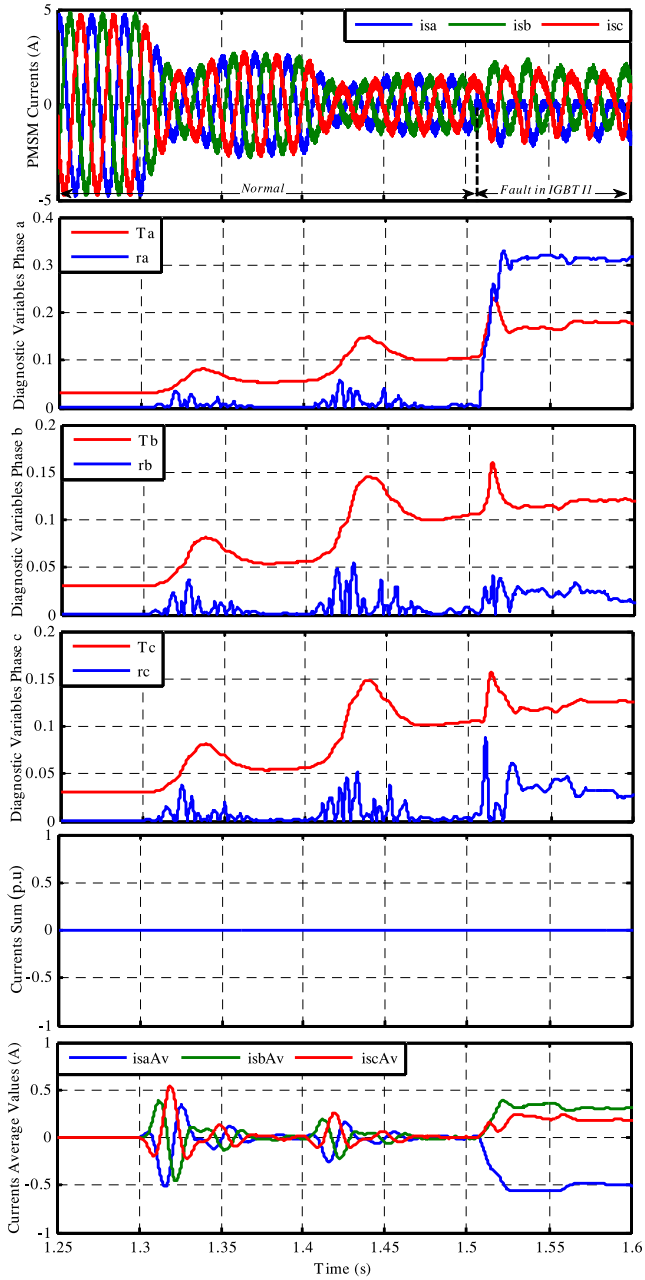

Fig. 5. Simulation results regarding the time-domain waveforms of the motor phase currents and the diagnostic variables, for an open-circuit fault in IGBT I1, a reference speed of 600 r/min and under load torque variations.

to diagnose multiple IGBTs open-circuit faults in the VSI, under 46% of the rated load torque and assuming a reference speed of 1340 r/min. A double power switch open-circuit fault occurs in IGBTs *I*5 and *I*1 at $t = 1.566$ and 1.64 s, respectively. The first fault in IGBT *I*5 leads to the increase in currents and higher harmonic distortion. This is even more pronounced after the second fault in *I*1. Due to the first fault, the residual r_b reaches its threshold T_b. Simultaneously, the current sum I_s remains at 0 and the value of i_{sbAv} becomes higher than $+T_o$. As a result, the inverter fault in IGBT *I*5 is detected and localized at the instant $t = 1.569$ s, which correspond to 33% of the currents period. Then, the *I*1 fault is identified 2 ms after the fault occurrence,

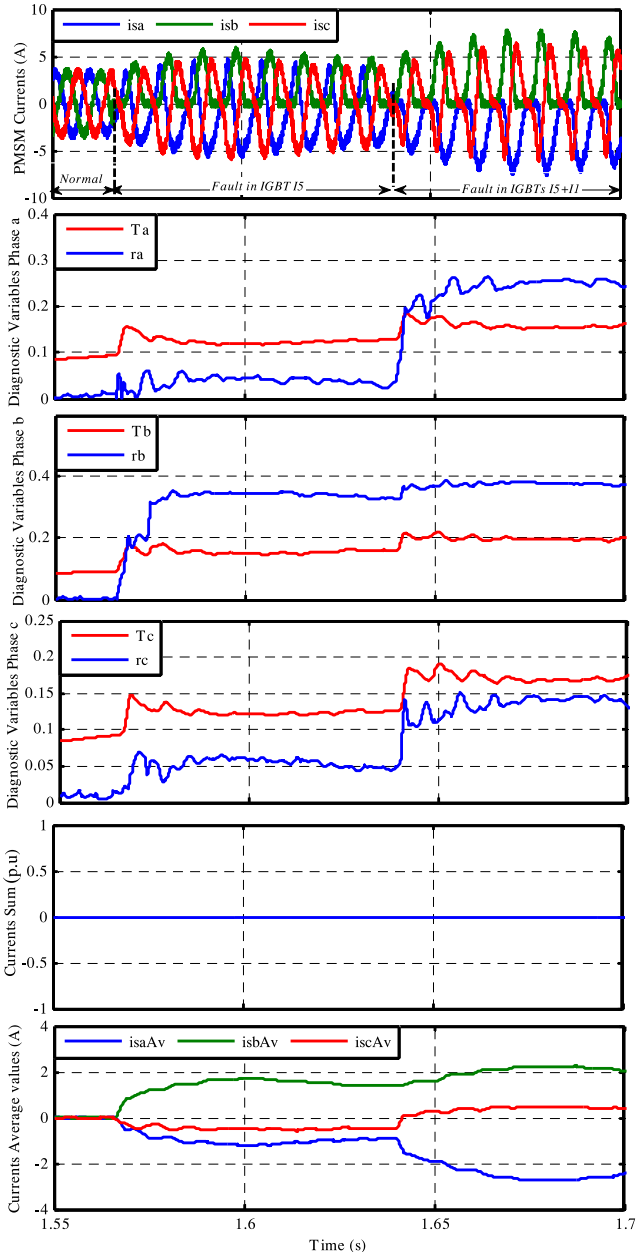

Fig. 6. Simulation results regarding the time-domain waveforms of the currents and the diagnostic variables, for a double open-circuit fault in IGBTs I1 and I5, a reference speed of 1340 r/min and under 46% of the rated load torque.

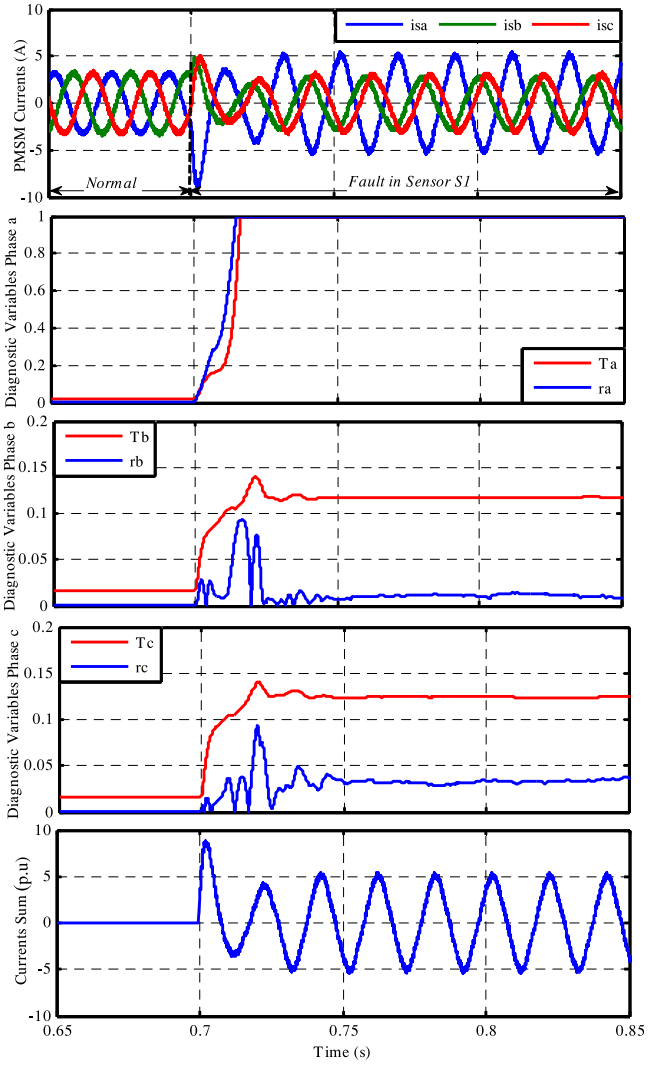

Fig. 7. Simulation results concerning the time-domain waveforms of the motor phase currents and the diagnostic variables, for a current sensor fault in S1, a reference speed of 600 r/min and 46% of the rated load torque.

when r_a crosses T_a, the current sum I_s remains zero and i_{saAv} diverges to a value below $-T_o$. In Fig. 7, a current sensor failure is considered, for a reference speed of 600 r/min and 46% of the rated load torque. At the instant $t = 0.7$ s, the $S1$ current sensor output of the motor phase "a" is forced to zero, and therefore, the control system receives the information that $i_{\mathrm{sa}} = 0$. Consequently, the current amplitude in this phase increases by a factor of $\sqrt{3}$, whereas the phase displacement between currents i_{sb} and i_{sc} decreases from 120° to 60°. Thereafter, high thermal and mechanical stresses occur in the motor. Regarding the fault diagnostic, the $S1$ fault is detected and localized at the instant $t = 0.701$ s, which corresponds to 5% of the motor currents period. This is accomplished when the residual r_a exceeds the adaptive threshold T_a and the current sum value I_s becomes null. It can be observed that the other residues corresponding to the healthy phases stay below their corresponding thresholds before and after the fault.

IV. Experimental Results

The experimental setup comprises basically a 2.2 kW PMSM coupled to an ac machine that is used as load, a Semikron SKiiP three-phase VSI, a dc bus capacitor bank of 2.35 mF, a diode bridge rectifier, and a dSPACE DS1103 digital controller. The used current sensors are the LEM LA 55-P. The PMSM parameters are the same as reported in Table II. The experimental setup is depicted in Figs. 8 and 9.

The RFOC control is combined with the SVM technique and applied to the VSI. The main control with the proposed fault diagnostic algorithm is implemented under MATLAB Simulink environment into the dSPACE DS1103 digital controller board

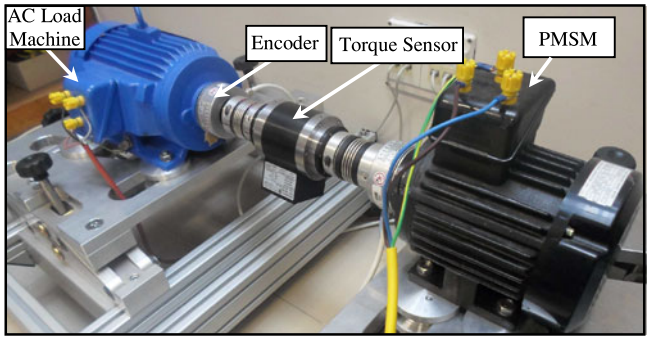

Fig. 8. Detail of the electric motor test bench.

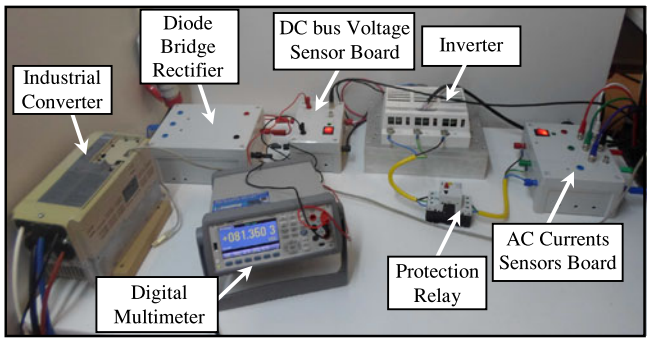

Fig. 9. General view of the power stages.

using a sampling time of 32 μs. The SVM switching frequency is defined to be of 6 kHz.

The same matrix gains L_1 and L_2, and threshold value T_o used for the simulation results were also used for the experimental validation.

A. Immunity to False Diagnostics

In Fig. 10, the performance of the proposed diagnostic algorithm under healthy operating conditions is addressed. A reference speed of 1340 r/min with load torque variations is considered. A time-varying load with an average load torque of 34% of the rated motor torque and an oscillating torque component with a frequency of 5 Hz are imposed.

As a consequence of the fast and strong unbalanced load torque imposed, the motor current oscillates within 16% and 50% of the rated motor current. The low-current values present a significant harmonic distortion, resulting in large oscillating diagnostic variables. The high-current values cause the decrease in the harmonic distortion, resulting in more stable diagnostic variables. Nevertheless, all residuals r_k remain near zero and far from their adaptive thresholds T_k. It can be seen that the defined adaptive thresholds can handle with their corresponding residuals without emitting false alarms, showing this way the algorithm immunity against false diagnostics, under these operating conditions.

B. Multiple IGBTs and Current Sensors Faults Diagnosis

Fig. 11 shows the experimental results of the motor currents together with the diagnostic variables, for a single power

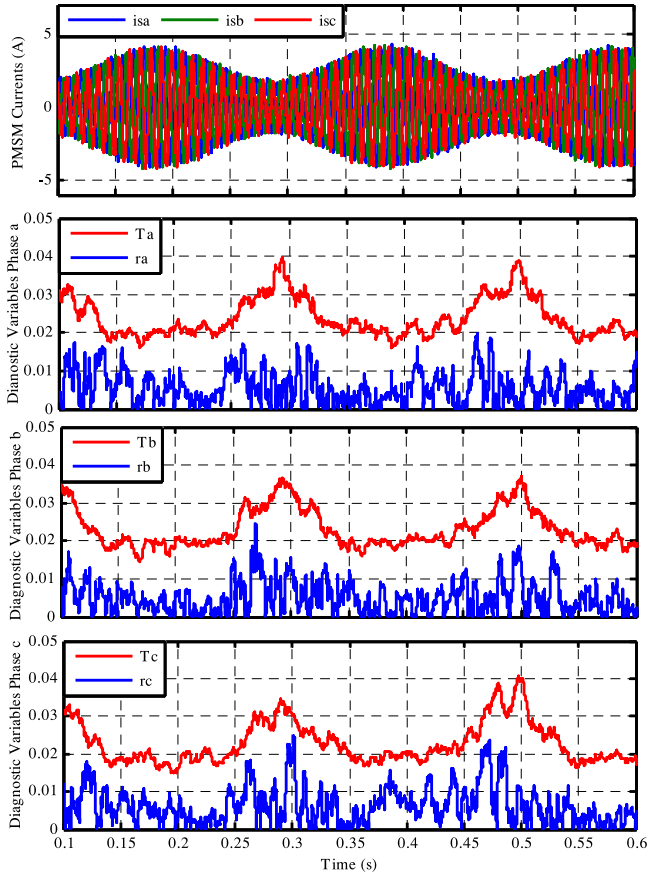

Fig. 10. Experimental results regarding the time-domain waveforms of the motor phase currents and the diagnostic variables, under a time-varying load and constant motor speed, for healthy operating conditions.

switch open-circuit fault in the IGBT *I*1, a reference speed of 1340 r/min, and load torque variations with an average load torque of 34% of the rated motor torque, and with a frequency of 5 Hz. Under healthy operating conditions and during the load transients, it can be seen that all residuals r_k stay always below their corresponding adaptive thresholds T_k and no false alarms are generated. At the instant $t = 0.607$ s, a failure occurs in IGBT *I*1. Meanwhile, the residual r_a increases above the adaptive threshold T_a, the currents sum I_s remains zero and the current average value i_{saAv} takes a negative value lower than the threshold $-T_o$, allowing for the localization of the faulty power switch *I*1. This happens 1 ms after the fault occurrence, corresponding to 11% of the fundamental currents period. In Fig. 12, a double power switch open-circuit fault in IGBTs *I*5 and *I*1 is considered. A constant reference speed of 600 r/min and a time-varying load with an average load torque of 25% of the rated motor torque, and an oscillating torque component with a frequency of 5 Hz are imposed. At the instant $t = 0.311$ s, the first fault is applied by removing the gate command signals to the IGBT *I*5. The faulty device is correctly localized at the instant $t = 0.316$ s (25% of the fundamental currents period), when the residual r_b crosses its adaptive threshold T_b, the currents sum I_s remains zero and the value of i_{sbAv} becomes higher than $+T_o$. Then, at $t = 0.611$ s, the gate command signal of the IGBT *I*1 is removed. Thereafter, at the instant $t = 0.62$ s, in a

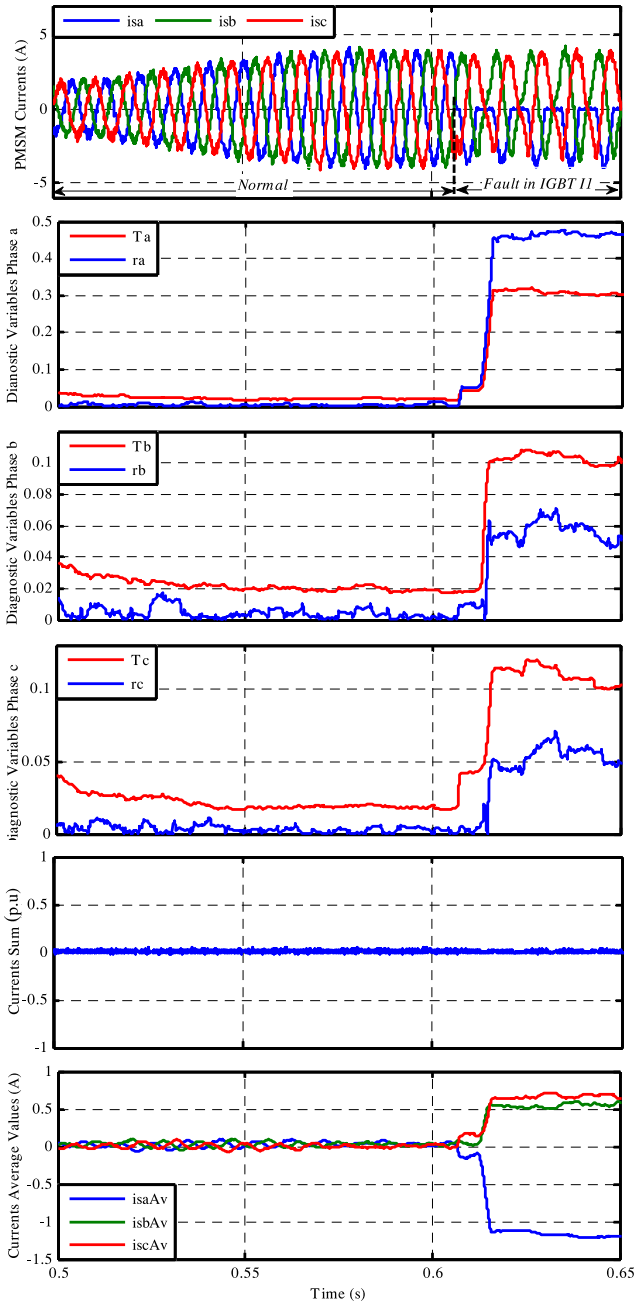

Fig. 11. Experimental results concerning the time-domain waveforms of the motor phase currents and the diagnostic variables, for an open-circuit fault in the IGBT I1, a reference speed of 1340 r/min and load torque variations.

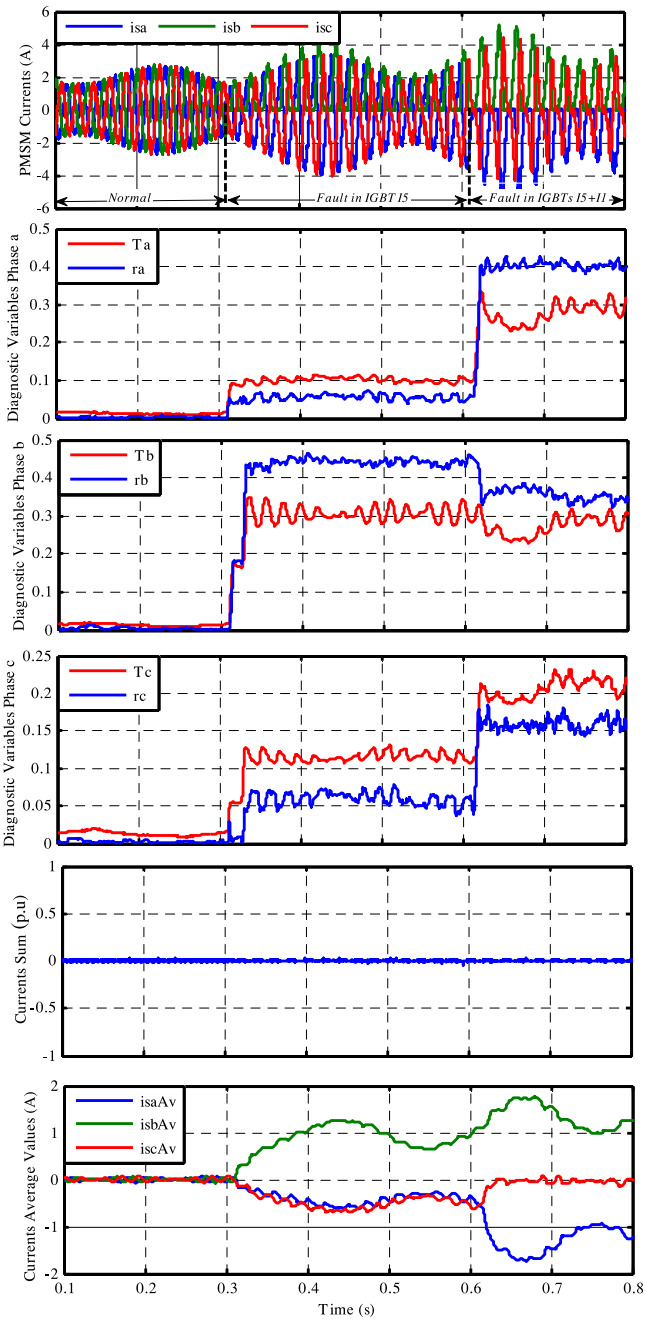

Fig. 12. Experimental results concerning the time-domain waveforms of the currents and the diagnostic variables, for a double open-circuit fault in IGBTs I5 and I1, under a reference speed of 600 r/min and load torque variations.

time interval of about 45% of the fundamental currents period, the r_a value reaches its threshold T_a and the value of i_{saAv} diverges to a value below $-T_o$, meaning that the $I1$ failure is successfully identified and showing that an effective diagnostic can be achieved under time-varying load conditions.

The PMSM currents together with the diagnostic variables are presented in Fig. 13, for a current sensor fault in PMSM phase currents, under 46% of the rated load torque and considering a reference speed of 600 r/min. The experimental current waveform is very similar to the one obtained from the computational simulations, shown in Fig. 7. Regarding the fault diagnosis, a current sensor fault is applied in $S1$ at the instant $t = 0.3$ s. Thereafter, the detection and identification of the failure are achieved at $t = 301$ s, corresponding to 5% of the fundamental currents period, when r_a reaches T_a and the currents sum I_s diverges from zero.

C. Fault Detection Times Versus Fault Inception Angles

Fig. 14 presents the average detection times for the proposed algorithm and for the algorithm proposed in [36], and considering a fault occurrence in IGBT $I1$ at different instants of phase

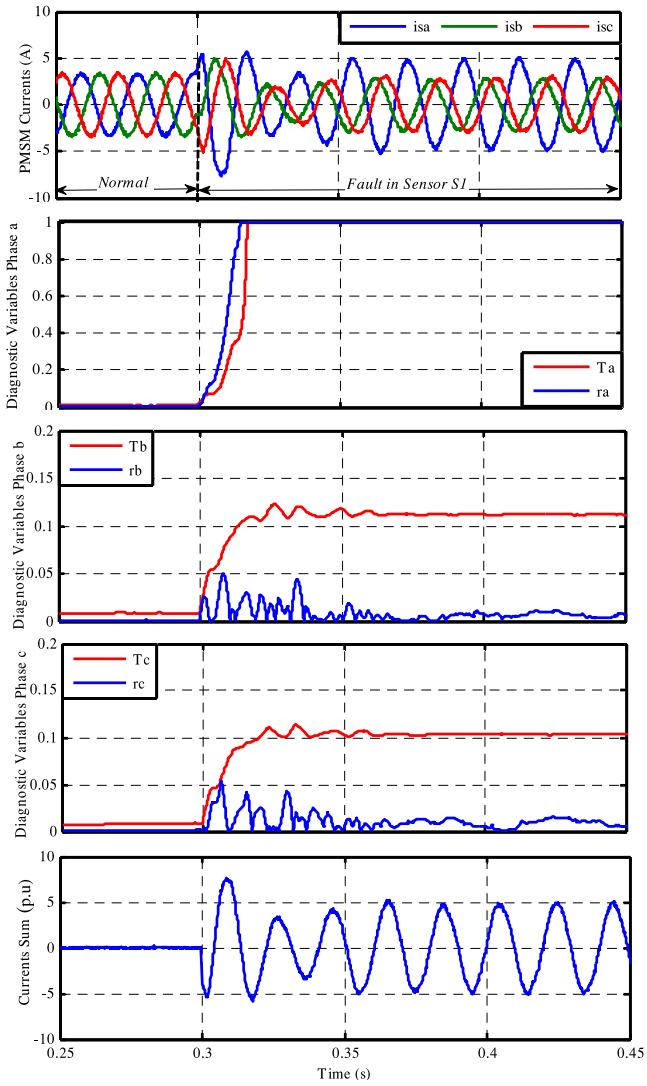

Fig. 13. Experimental results concerning the time-domain waveforms of the motor phase currents and the diagnostic variables, for a current sensor fault in S1, under a reference speed of 600 r/min and 46% of the rated load torque.

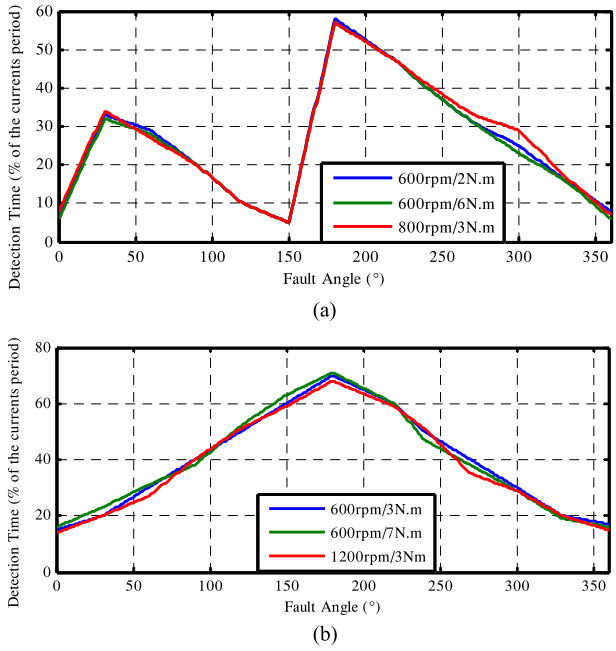

Fig. 14. Average detection times of a single open-circuit fault in IGBT *I*1 by using (a) the proposed algorithm and (b) the method proposed in [36].

"a" current, under distinct operating points. It is clear from Fig. 14(a) that the proposed fault diagnostic algorithm has a detection time between 5% and 58% of the current fundamental period, depending on the fault angle.

As the opened IGBT *I*1 affects only the positive current half-cycle in the phase "a," the fault can be detected in that half-cycle if the fault angle is within the interval 0° and 170°. Otherwise, the algorithm will detect the fault in the next positive current half-cycle. The fault diagnostic method proposed in [36] has a detection time between 15% and 71% of the current fundamental period [see Fig. 14(b)]. Furthermore, the proposed fault diagnostic algorithm is not limited to detect and localize multiple IGBT open-circuit faults, being also capable to diagnose current sensor faults. The current sensor fault detection is performed within fast detection times (≈5% of the motor currents period, independent of the fault angle). Therefore, it can be concluded that the proposed fault diagnostic algorithm presents good fault detection times with respect to power switch open-circuit faults as well as current sensor faults. Therefore, the proposed technique can be effectively utilized for triggering post-fault remedial strategies in fault-tolerant drives.

V. Conclusion

In this paper, a single fault diagnostic approach has been proposed for multiple IGBTs open-circuit faults and current sensor failures in PMSM drives, requiring only the information available from the main control system, without using additional hardware requirements. The method is based on residual generation, using observed and measured stator currents, to compute the value of CFF. The sensitivity and robustness of the proposed method depend strictly on the defined thresholds. Therefore, an adaptive threshold method has been investigated; it depends on the observer error and the average value of the current. Taking into account the transient and steady-state modes, the evolution of the generated residuals together with their corresponding thresholds is used to detect a fault occurrence. Then, IGBTs faults can be distinguished from current sensors faults using the currents sum, and the IGBT fault isolation can be easily accomplished through the current average values.

Simulations and experimental results demonstrate the robustness and effectiveness of the proposed method under different operating points and distinct faulty scenarios. Due to the use of adaptive thresholds, the technique presents a very high immunity against false alarms in healthy mode, independent of the system operating point. Simultaneously, the technique allows for the diagnostics of both multiple IGBTs open-circuits faults and current sensors faults with low detection times.

REFERENCES

[1] V. Smet *et al.*, "Ageing and failure modes of IGBT modules in high-temperature power cycling," *IEEE Trans. Ind. Electron.*, vol. 58, no. 10, pp. 4931–4941, Oct. 2011.

[2] H. Schwab, A. Klonne, S. Reck, and I. Rameshold, "Reliability evaluation of a permanent magnet synchronous motor drive for an automotive application," in *Proc. Conf. Rec. 10th Eur. Power Electron. Appl. Conf.*, Toulouse, France, 2003, pp. 1–10.

[3] S. Yang, A. Bryant, P. Mawby, D. Xiang, L. Ran, and P. Tavner, "An industry-based survey of reliability in power electronic converters," *IEEE Trans. Ind. Appl.*, vol. 47, no. 3, pp. 1441–1451, May/Jun. 2011.

[4] D. Kastha and B. K. Bose, "Investigation of fault modes of voltage-fed inverter system for induction motor drive," *IEEE Trans. Ind. Appl.*, vol. 30, no. 4, pp. 1028–1038, Jul./Aug. 1994.

[5] S. Yang, D. Xiang, A. Bryant, P. Mawby, L. Ran, and P. Tavner, "Condition monitoring for device reliability in power electronic converters: A review," *IEEE Trans. Power Electron.*, vol. 25, no. 11, pp. 2734–2752, Nov. 2010.

[6] D. U. Campos-Delgado, E. Palacios, and D. R. Espinoza-Trejo, "Fault-tolerant control in variable speed drives: A survey," *IET Electr. Power Appl.*, vol. 2, no. 2, pp. 121–134, Mar. 2008.

[7] G. Betta and A. Pietrosanto, "Instrument fault detection and isolation: State of the art and new research trends," *IEEE Trans. Instrum. Meas.*, vol. 49, no. 1, pp. 100–107, Feb. 2000.

[8] U. M. Choi, F. Blaabjerg, and K. B. Lee, "Study and handling methods of power IGBT module failures in power electronic converter systems," *IEEE Trans. Power Electron.*, vol. 30, no. 5, pp. 2517–2533, May 2015.

[9] L. Bin and S. K. Sharma, "A literature review of IGBT fault diagnostic and protection methods for power inverters," *IEEE Trans. Ind. Appl.*, vol. 45, no. 5, pp. 1770–1777, Sep./Oct. 2009.

[10] K. Rothenhagen and F. W. Fuchs, "Performance of diagnosis methods for IGBT open circuit faults in voltage source active rectifiers," in *Proc. 35th Power Electron. Spec. Conf.*, Aachen, Germany, 2004, pp. 4348–4354.

[11] K. Rothenhagen and F. W. Fuchs, "Performance of diagnosis methods for IGBT open circuit faults in three phase voltage source inverters for ac variable speed drives," in *Proc. Eur. Conf. Power Electron. Appl.*, vol. 10, 2005, pp. 1–10.

[12] W. Sleszynski, J. Nieznanski, and A. Cichowski, "Open-transistor fault diagnostics in voltage-source inverters by analyzing the load currents," *IEEE Trans. Ind. Electron.*, vol. 56, no. 11, pp. 4681–4688, Nov. 2009.

[13] M. Trabelsi, M. Boussak, and M. Gossa, "Multiple IGBTs open circuit faults diagnosis in voltage source inverter fed induction motor using modified slope method," in *Proc. 19th Int. Conf. Electr. Mach.*, vol. 6, Sep. 2010, pp. 6–8.

[14] C. Cecati, A. O. Di Tommaso, F. Genduso, R. Miceli, and G. R. Galluzzo "Comprehensive modeling and experimental testing of fault detection and management of a non redundant fault-tolerant VSI," *IEEE Trans. Ind. Electron.*, vol. 62, no. 6, pp. 3945–3954, Jun. 2015.

[15] F. Wu and J. Zhao, "Current similarity analysis based open-circuit fault diagnosis for two-level three-phase PWM rectifier," *IEEE Trans. Power Electron*, (Early Access), 2016.

[16] S. Khomfoi and L. M. Tolbert, "Fault diagnostic system for a multilevel inverter using a neural network," *IEEE Trans. Power Electron.*, vol. 22, no. 3, pp. 1062–1069, May 2007.

[17] F. Zidani, D. Diallo, M. E. H. Benbouzid, and R. Naït-Saïd, "A fuzzy based approach for the diagnosis of fault modes in a voltage-fed PWM inverter induction motor drive," *IEEE Trans. Ind. Electron.*, vol. 55, no. 2, pp. 586–593, Feb. 2008.

[18] M. Aktas and V. Turkmenoglu, "Wavelet-based switching faults detection in direct torque control induction motor drives," *IET Sci., Meas. Technol.*, vol. 4, no. 6, pp. 303–310, Nov. 2010.

[19] H. B. A. Sethom and M. A. Ghedamsi, "Intermittent misfiring default detection and localisation on a PWM inverter using wavelet decomposition," *J. Electr. Syst.*, vol. 4, no. 2, pp. 222–234, 2008.

[20] C. Gan, J. Wu, S. Yang, Y. Hu, and W. Cao, "Wavelet packet decomposition-based fault diagnosis scheme for SRM drives with a single current sensor," *IEEE Trans. Energy Convers.*, vol. 31, no. 1, pp. 303–313, Mar. 2016.

[21] J. O. Estima, N. M. A. Freire, and A. J. M. Cardoso, "Recent advances in fault diagnosis by Park's vector approach," in *Proc. IEEE Workshop Electr. Mach. Design, Control Diagnosis*, Mar. 2013, pp. 279–288.

[22] J. O. Estima and A. J. M. Cardoso, "A new approach for real-time multiple open-circuit fault diagnosis in voltage source inverters," *IEEE Trans. Ind. Appl.*, vol. 47, no. 6 pp. 2487–2494, Nov. 2011.

[23] J. O. Estima and A. J. M. Cardoso, "A new algorithm for real-time multiple open-circuit fault diagnosis in voltage-fed PWM motor drives by the reference current errors," *IEEE Trans. Ind. Electron.*, vol. 60, no. 8, pp. 3496–3505, Aug. 2013.

[24] D. Diallo, M. E. H. Benbouzid, D. Hamad, and X. Pierre, "Fault detection and diagnosis in an induction machine drive: A pattern recognition approach based on concordia stator mean current vector," *IEEE Trans. Energy Convers.*, vol. 20, no. 3, pp. 512–519, Sep. 2005.

[25] D. U. Campos-Delgado, J. A. Pecina-Sanchez, D. R. Espinoza-Trejo, and E. R. Arce-Santana, "Diagnosis of open-switch faults in variable speed drives by stator current analysis and pattern recognition," *IET Electr. Power Appl.*, vol. 7, no. 6, pp. 509–522, Jul. 2013.

[26] R. L. A. Ribeiro, C. B. Jacobina, E. R. C. Silva, and A. M. N. Lima, "Fault detection of open-switch damage in voltage-fed PWM motor drive systems," *IEEE Trans. Power Electron.*, vol. 18, no. 2, pp. 587–593, Mar. 2003.

[27] Q.-T. An, L.-Z. Sun, and T. M. Jahns, "Low-cost diagnostic method for open-switch faults in inverters," *Electron. Lett.*, vol. 46, no. 14, pp. 1021–1022, Jul. 2010.

[28] M. A. Rodríguez-Blanco, A. Vazquez Pérez, L. Hernández-González, V. Golikov, J. Aguayo-Alquicira, and M. May-Alarcon, "Fault detection for IGBT using adaptive thresholds during the turn-on transient," *IEEE Trans. Ind. Electron.*, vol. 62, no. 3, pp. 1975–1983, Mar. 2015.

[29] C. Shu, C. Ya-Ting, Y. Tian-Jian, and W. Xun, "A novel diagnostic technique for open-circuited faults of inverters based on output line-to-line voltage model" *IEEE Trans. Ind. Electron.*, vol. 63, no. 7, pp. 4412–4421, Jul. 2016.

[30] B. Gou, X. Ge, S. Wang, X. Feng, J. B. Kuo, and T. G. Habetler, "An open-switch fault diagnosis method for single-phase PWM rectifier using a model-based approach in high-speed railway electrical traction drive system," *IEEE Trans. Power Electron.*, vol. 31, no. 5, pp. 3816–3826, May 2016.

[31] N. M. A. Freire, J. O. Estima, and A. J. M. Cardoso, "A voltage-based approach without extra hardware for open-circuit fault diagnosis in closed-loop PWM AC regenerative drives," *IEEE Trans. Ind. Electron.*, vol. 61, no. 9, pp. 4960–4970, Mar. 2014.

[32] S. M. Jung, J. S. Park, H. W. Kim, K. W. Cho, and M. J Youn, "An MRAS-based diagnosis of open-circuit fault in PWM voltage-source inverters for PM synchronous motor drive systems," *IEEE Trans. Power Electron.*, vol. 28, no. 5, pp. 2514–2526, May 2013.

[33] D. U. Campos-Delgado and D. R. Espinoza-Trejo, "An observer-based diagnosis scheme for single and simultaneous open-switch faults in induction motor drives," *IEEE Trans. Ind. Electron.*, vol. 58, no. 2, pp. 671–679, Feb. 2011.

[34] D. R. Espinoza-Trejo, D. U. Campos-Delgado, G. Bossio, E. Barcenas, J. E. Hernandez-Diez, and L. F. Lugo-Cordero, "Fault diagnosis scheme for open-circuit faults in field-oriented control induction motor drives," *IET Power Electron.*, vol. 6, no. 5, pp. 869–877, May 2013.

[35] Q. T. An, L. Sun, and L. Z. Sun, "Current residual vector-based open-switch fault diagnosis of inverters in PMSM drive systems," *IEEE Trans. Power Electron.*, vol. 30, no. 5, pp. 2814–2827, May 2015.

[36] I. Jlassi, J. O. Estima, S.K. El Khil, N. M. Bellaaj, and A. J. M. Cardoso, "Multiple open-circuit faults diagnosis in back-to-back converters of PMSG drives for wind turbine systems," *IEEE Trans. Power Electron.*, vol. 30, no. 5, pp. 2689–2702, May 2015.

[37] D. W. Chung and S. K. Sul, "Analysis and compensation of current measurement error in vector-controlled AC motor drives," *IEEE Trans. Ind. Appl.*, vol. 34, no. 2, pp. 340–345, Mar./Apr. 1998.

[38] H.-S. Jung, S.-H. Hwang, J.-M. Kim, C.-U. Kim, and C. Choi, "Diminution of current measurement error for vector controlled AC motor drives," *IEEE Trans. Ind. Appl.*, vol. 42, no. 5, pp. 1249–1256, Sep./Oct. 2006.

[39] K. Rothenhagen and F.W. Fuchs, "Doubly fed induction generator modelbased sensor fault detection and control loop reconfiguration," *IEEE Trans. Ind. Electron.*, vol. 56, no. 10, pp. 4229–4238, Oct. 2009.

[40] K. Rothenhagen and F. W. Fuchs, "Current sensor fault detection, isolation, and reconfiguration for doubly fed induction generators," *IEEE Trans. Ind. Electron.*, vol. 56, no. 10, pp. 4239–4245, Oct. 2009.

[41] S. Karimi, A. Gaillard, P. Poure, and S. Saadate, "Current sensor fault tolerant control for WECS with DFIG," *IEEE Trans. Ind. Electron.*, vol. 56, no. 11, pp. 4660–4670, Nov. 2009.

[42] M. Merai, M. W. Naouar, I. Slama-Belkhodja, and E. Monmasson, "FPGA-based fault tolerant space vector hysteresis current control for three-phase grid connected converter," *IEEE Trans. Ind. Electron.*, vol. 63, no. 11, pp. 7008–7017, Nov. 2016.

[43] H. Berriri, M. W. Naouar, and I. Slama-Belkhodja, "Easy and fast sensor fault detection and isolation algorithm for electrical drives," *IEEE Trans. Power Electron.*, vol. 27, no. 2, pp. 490–499, Feb. 2012.
[44] A. Ben Youssef, S. K. El Khil, and I. Slama-Belkhodja, "State observer-based sensor fault detection and isolation, and fault tolerant control of a single-phase PWM rectifier for electric railway traction," *IEEE Trans. Power Electron.*, vol. 28, no. 12, pp. 5842–5853, 2013.
[45] Y. Jeong, S. Sul, S. E. Schulz, and N. R. Patel, "Fault detection and fault-tolerant control of interior permanent-magnet motor drive system for electric vehicle," *IEEE Trans. Ind. Appl.*, vol. 41, no. 1, pp. 46–51, Jan./Feb. 2005.
[46] T. A. Najafabadi, F. R. Salmasi, and P. J. Maralani, "Detection and isolation of speed-, DC-link voltage-, and current-sensor faults based on an adaptive observer in induction-motor drives," *IEEE Trans. Ind. Electron.*, vol. 58, no. 5, pp. 1662–1672, May 2011.
[47] G. H. B. Foo, X. Zhang, and B. M. Vilathgamuwa, "A novel speed, DC-link voltage and current sensor fault detection and isolation in IPM synchronous motor drives using an extended Kalman filter," *IEEE Trans. Ind. Electron.*, vol. 60, no. 8, pp. 3485–3495, Aug. 2013.
[48] A. Akrad, M. Hilairet, and D. Diallo, "Design of a fault-tolerant controller based on observers for a PMSM drive," *IEEE Trans. Ind. Electron.*, vol. 58, no. 4, pp. 1416–1427, Apr. 2011.
[49] B. Tabbache, M. Benbouzid, A. Kheloui, and J. M. Bourgeot, "Virtual sensor-based maximum likelihood voting approach for fault-tolerant control of electric vehicle powertrains," *IEEE Trans. Veh. Technol.*, vol. 62, no. 3, pp. 1075–1083, Mar. 2013.
[50] C. Chakraborty and V. Verma, "Speed and current sensor fault detection and isolation technique for induction motor drive using axes transformation," *IEEE Trans. Ind. Electron.*, vol. 62, no. 3, pp. 1943–1953, Mar. 2015.
[51] N. M. A. Freire, J. O. Estima, and A. J. M. Cardoso, "A new approach for current sensor fault diagnosis in PMSG drives for wind energy conversion systems," *IEEE Trans. Ind. Appl.*, vol. 50, no. 2, pp. 1206–1214, Mar./Apr. 2014.
[52] S. K. El Khil, I. Jlassi, J. O. Estima, N. Mrabet Bellaaj, and A. J. M. Cardoso, "Current sensor fault detection and isolation method for PMSM drives, using average normalised currents," *IET Electron. Lett.*, vol. 52, no. 17, pp. 1434–1436, Aug. 2016.
[53] A. Abdullah and M. Zribi, "Sensor-fault-tolerant control for a class of linear parameter varying systems with practical examples," *IEEE Trans. Ind. Electron.*, vol. 60, no. 11, pp. 5239–5251, Nov. 2013.

Imed Jlassi was born in Tunis, Tunisia, in 1984. He received the B.S., M.S., and Ph.D. degrees in electrical engineering from the École Nationale d'Ingénieurs de Tunis, Laboratoire des Systèmes Électriques (LR11ES15), Tunis, Tunisia, in 2009, 2011, and 2016, respectively.

In January 2014, he joined the Electromechatronic Systems Research Centre (http://www.cise.ubi.pt), University of Beira Interior, Covilhã, Portugal. His main research interests include drive control of electric machines, fault diagnosis, and fault-tolerant control of ac motors drives and wind turbine systems.

Jorge O. Estima (S'08–M'10) was born in Aveiro, Portugal, in 1984. He received the E. E. diploma and the Ph.D. degree in fault-tolerant electric drives from University of Coimbra, Coimbra, Portugal, in 2007 and 2012, respectively.

Since then, he has been a Postdoctoral Researcher in CISE—Electromechatronic Systems Research Centre, University of Beira Interior, Covilhã, Portugal. His research interests include condition monitoring and diagnostics of power electronics and AC motors, fault-tolerant variable speed drives, and energy efficiency in motor drive systems.

Sejir Khojet El Khil was born in Tunis, Tunisia, in 1977. He received the Diploma degree in electrical engineering from the Ecole Nationale d'Ingénieurs de Tunis (ENIT), Tunis, Tunisia, in 2001, the Ph.D. degree from ENIT and the Ecole Nationale Polytechnique de Toulouse-France in 2006 and the Habilitation degree in electrical engineering from ENIT in 2016.

Since 2008, he has been a permanent Researcher with the Université de Tunis El Manar, ENIT, Laboratoire des Systèmes Electriques (LSE–LR11ES15), and an Assistant Professor at the Institut Supérieur des Etudes Technologiques en Communication de Tunis (Iset'Com), Tunisia. In January 2014, he joined the CISE—Electromechatronic Systems Research Centre, University of Beira Interior, Covilha, Portugal, as a Ph.D. Collaborator. His main research interests include fault detection and fault tolerant control of electrical drives and telecom power supply.

Najiba Mrabet Bellaaj received the Diploma degree in electrical engineering in 1988 and the Ph.D. degree in electrical engineering from the École Nationale d'Ingénieurs de Tunis, Laboratoire des Systèmes Électriques, Tunis, Tunisia, in 2001. She received the "Habilitation" Diploma degree in electrical engineering from ENIT in 2011.

She was an Assistant Professor at Institut Superieur d'Informatique d'EL Manar in 2011. Since 2011, she has been an Associate Professor in ISI. She became an Associate Professor at the same institute. She did her research in Electrical System Laboratory (LR-11-ES15), Ecole Nationale d'Ingenieurs de Tunis, Tunisia. Her research interests include intelligent techniques, electrical machines, modeling, diagnosis, renewable energy, and smart grids.

Antonio J. Marques Cardoso (S'89–A'95–SM'99) received the Dipl. Eng., Dr. Eng., and Habilitation degrees from the University of Coimbra, Coimbra, Portugal, in 1985, 1995, and 2008, respectively, all in electrical engineering.

From 1985 until 2011, he was with the University of Coimbra, Coimbra, Portugal, where he was the Director of the Electrical Machines Laboratory. Since 2011, he has been with the University of Beira Interior (UBI), Covilhã, Portugal, where he is a Full Professor in the Department of Electromechanical Engineering and the Director of Electromechatronic Systems Research Centre (http://cise.ubi.pt). He was a Vice-Rector of the UBI, in 2013–2014. He is the author of a book entitled *Fault Diagnosis in Three-Phase Induction Motors* (Coimbra, Portugal: Coimbra Editora, 1991) (in Portuguese) and of approximately 400 papers published in technical journals and conference proceedings. His current research interests include fault diagnosis and fault tolerance in electrical machines, power electronics, and drives.

Dr. Cardoso serves as a Guest Editor of the IEEE TRANSACTIONS ON INDUSTRY APPLICATIONS Special Issue on Fault Diagnosis of Electric Machines, Power Electronics and Drives, and an Associate Editor for the IEEE TRANSACTIONS ON INDUSTRY APPLICATIONS, the IEEE TRANSACTIONS ON INDUSTRIAL ELECTRONICS, the IEEE JOURNAL OF EMERGING AND SELECTED TOPICS IN POWER ELECTRONICS, and *Springer International Journal of Systems Assurance Engineering and Management*.